International Journal of Geosynthetics and Ground Engineering (2017) 3:39
https://doi.org/10.1007/s40891-017-0116-4

ORIGINAL PAPER

Effect of Seasonal Changes on a Hybrid Soil–Geofoam Embankment System

Ali Shafikhani[1] · Tejo V. Bheemasetti[1] · Anand J. Puppala[1]

Received: 29 September 2017 / Accepted: 8 November 2017 / Published online: 29 November 2017

Abstract
The effects of climatic variations on the performance of the bridge infrastructure were not adequately addressed. This paper presents a comprehensive analysis of the effect of seasonal temperature and precipitation variations on a bridge infrastructure located in Johnson County, Texas. This bridge has undergone a rehabilitation process by partially replacing the embankment soil with lightweight expanded polystyrene geofoam (EPS geofoam) to reduce bridge approach slab settlements. Four years of monitored vertical deformation and pressure cell data from the field instrumentation was used to analyze the performance of the bridge slab and adjoining roadway pavement system. From the analysis, it was observed that the vertical pressures and total deformations were increased with an increase in temperature and were decreased with a decrease in temperature. Also, with an increase in the temperature, it was observed that the bridge retaining wall exerted lateral pressure on the geofoam blocks and with a decrease in temperature the pressures decreased considerably. This study highlights the observations made on the bridge approach slab and adjoining roadway pavement vertical deformations with respect to temperature and precipitation variations.

Keywords Seasonal changes · Vertical movements · Pressures · EPS geofoam

Introduction and Background

The bump at the end of a bridge is a phenomenon in which the bridge approach slab experiences differential settlement in relation to the bridge deck and the adjoining roadway pavement [1–5]. In the United States, approximately 28 states use approach slabs as an interface between the pavement and the bridge deck. Out of these 28 States, 7 States use this system in 100% of their bridges, 12 States use it in more than 75% of their bridges, 4 States use it in 50–75% of their bridges, and 4 States use this system in 25–50% of their bridges [6]. Approximately 25% of the 600,000 bridges in the United States have encountered the bump problem, and millions of dollars were spent annually for the repair costs [2, 7]. A particular survey revealed that it costs annually more than 100 million dollars for Texas Department of Transportation (TxDOT) to repair all the bridges with bump problem in Texas [8].

The primary factors causing bump phenomenon include poor soil compaction, soil erosion, water infiltration beneath the pavement, development of voids, and settlement of backfill material due to excessive overburden pressure [2–5, 9–25]. To mitigate this problem, several techniques such as excavation and replacement of fill material, deep soil mixing (DSM) columns, geosynthetic reinforcement, mechanically stabilized earth (MSE) wall, lightweight EPS geofoam replacement, effective drainage, and erosion control methods were recommended [5, 9, 11, 13, 14, 20, 22–32]. Although several techniques were discussed on the mitigation of bump phenomenon, the effect of differential settlement impulse factors such as climatic variations on the performance of the bridge infrastructure were not addressed sufficiently.

The main objective of this research is to study the influence of temperature and precipitation on the pressures and vertical deformations subjected on a soil–geofoam bridge approach slab embankment. In the past decade, researchers have performed many laboratory studies to determine

✉ Anand J. Puppala
anand@uta.edu

Ali Shafikhani
ali.shafikhani@mavs.uta.edu

Tejo V. Bheemasetti
tejovikash.bheemasetti@mavs.uta.edu

[1] Department of Civil Engineering, The University of Texas at Arlington, Box 19308, Arlington, TX 76019, USA

the thermal properties of geofoam material [33–36]. It was observed that the compressive strength of geofoam material decreases with an increase in the temperature [37]. The following sections provide the details of the test site, in-situ instrumentation, and data analysis.

Site Description

The US 67 bridge constructed over SH 174 located in Johnson County, Cleburne, Texas was considered in this study. The abutments at the ends of the bridge are supported on drilled shaft foundations. The bridge approach slab was constructed on 12.2 m (40 ft) high embankment to connect the bridge deck and the roadway pavement. Since its construction in 1995, the approach slab has undergone more than 406.4 mm (16 in.) of settlement [1, 38]. Several mitigation measures such as soil nailing, grout injections, and hot mix overlays were attempted to mitigate the bump phenomenon. However, none of the techniques provided satisfactory performance [1].

In January 2012, the Texas Department of Transportation (TxDOT) Fort Worth District chose lightweight EPS22 geofoam as a replacement embankment fill material to reduce the overburden stresses as well as the erosion of the backfill material. The EPS22 was selected based on the calculations of stresses from the traffic load, construction equipment, and pavement surcharge. Table 1 presents the physical properties of the EPS22 geofoam [39].

Based on the vertical pressures from the traffic load, construction equipment, and pavement surcharge, it was determined that replacing the embankment soil for the top 1.83 m (6 ft) would suffice the technical requirements. With EPS geofoam density of 21 kg/m^3 compared to traditional fill material with approximately 1937–2040 kg/m^3, the overburden stress was reduced by 100 times compared to traditional fill material. Approximately 1177 cubic yards of EPS22 geofoam was used in this project to replace the top 1.83 m (6 ft) of embankment soil. The geofoam material stacked in three layers was wrapped using an impermeable geomembrane to resist infiltration of chemical liquids and petroleum solvents.

Table 1 Physical properties of EPS22 geofoam

Property description	Quantity
Density (kg/m^3)	21.6
Compressive resistance at 1% deformation (kPa)	50
Compressive resistance at 5% deformation (kPa)	115
Compressive resistance at 10% deformation (kPa)	135
Flexural strength (kPa)	276
Oxygen index (vol%)	24
Water absorption (vol% max)	3

On top of the geofoam layer, a 0.61 m (2 ft) pavement structure consisting of a 0.25 m (10 in.) aggregate flexible base, 0.10 m (4 in.) Hot mix asphalt concrete (HMAC), and 0.25 m (10 in.) concrete pavement was constructed. In order to evaluate the performance of the geofoam as an embankment material, the test site was instrumented as illustrated in the following sections.

Instrumentation and Database

The test site was instrumented to evaluate the performance of the geofoam as an embankment material. Four horizontal inclinometer casings (US67-1, US67-2, US67-3, and US67-4) were installed on the top of the geofoam to measure the vertical deformations as illustrated in Fig. 1. Additionally, to monitor vertical and lateral pressures at the top, bottom, and sides of the geofoam, four pressure cells equipped with thermometers were installed. Figure 2a, b show the pressure cells installed at the top and bottom of the geofoam blocks to measure the vertical pressures. Figure 2c, d show the pressure cells installed on the abutment and the wing

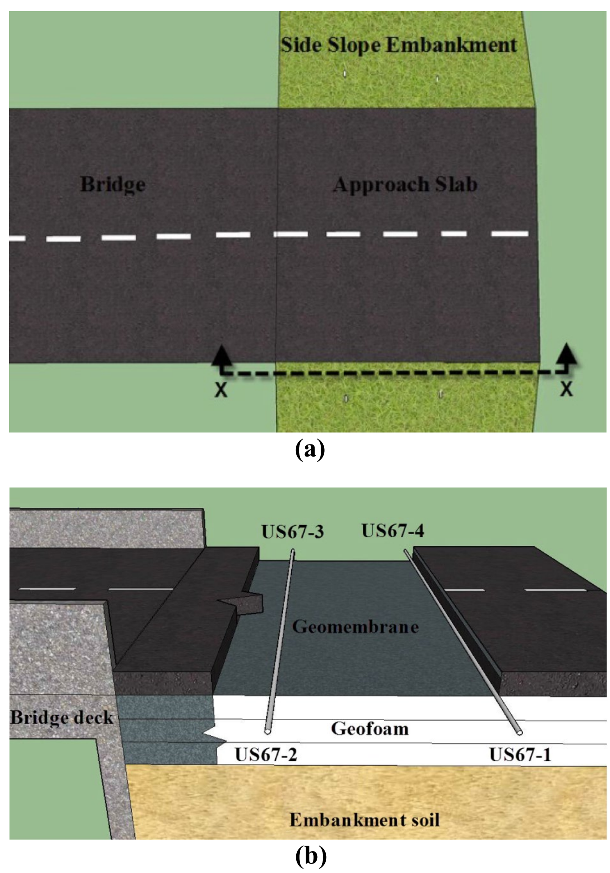

Fig. 1 Soil–geofoam-bridge at US 67: **a** top view; **b** cross-section view

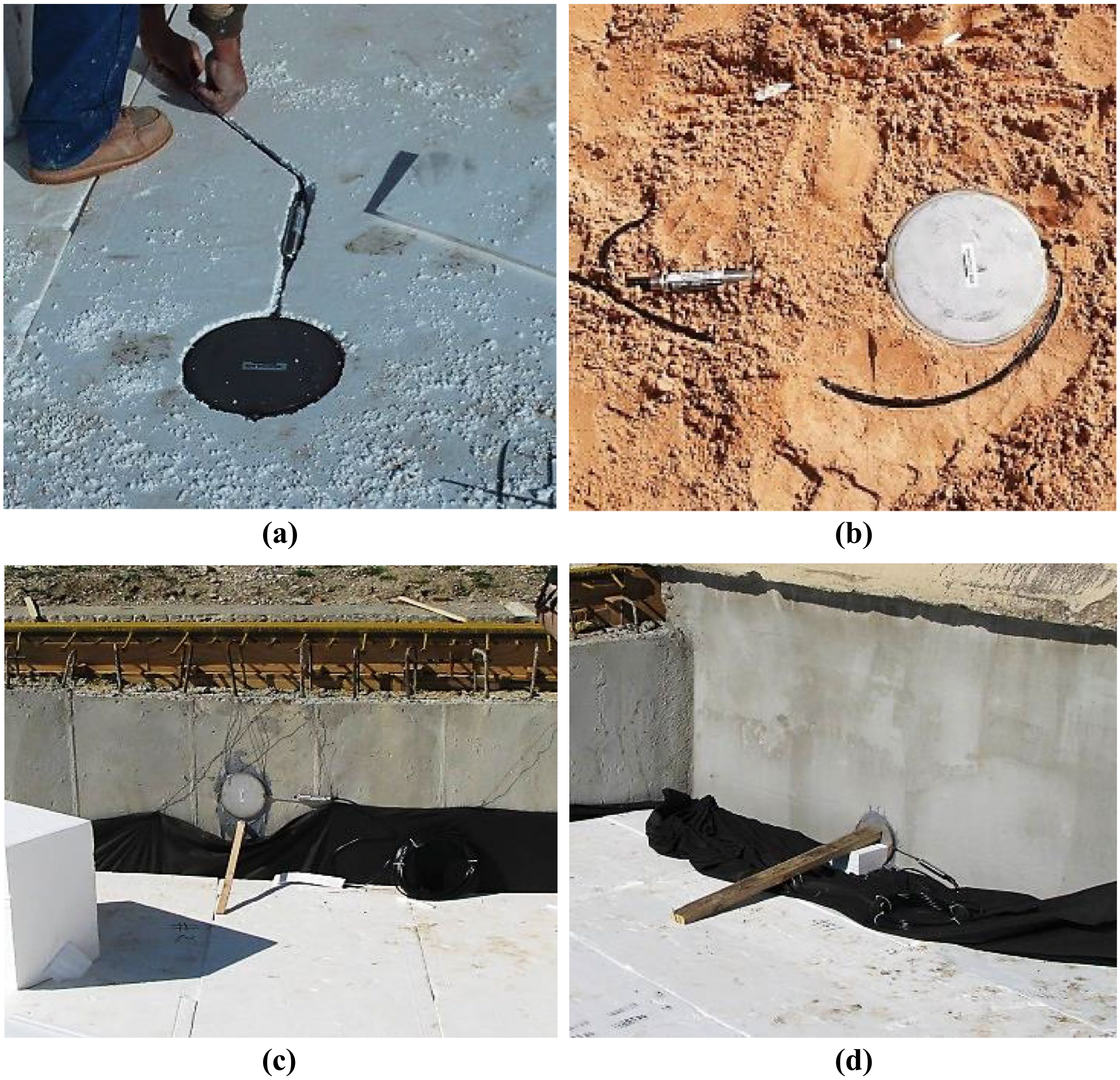

Fig. 2 Four pressure cells installed at the bridge approach slab: **a**, **b** vertical pressure cells; **c**, **d** lateral pressure cells

wall to measure the lateral pressures. The pressure cells were connected to a Quattro logger, which was set to record the readings for each 15-min time interval. It shall be noted that the VW Quattro Logger's electronics are impervious to humidity and condensation, which is rated to collect reliable data from − 20 to + 70 °C [40].

It was observed that the soil–geofoam bridge embankment has undergone < 38.1 mm (1.5 in.) of differential settlement over 4-year time period. The threshold limits for bump phenomenon varies for different agencies which can be found elsewhere [1]. The lateral pressure cell installed on the inside wall of the bridge abutment showed occasional negative values. Whereas, the pressure cell installed at the bottom of the inside of the north wing wall stopped working properly, which could be due to loss of contact with the geofoam layer. These observations led researchers to analyze the physical interaction between the abutment and wing wall and the geofoam layer due to temperature variations. The following sections present the analyses performed on the pressures and vertical deformations of the approach slab and bridge infrastructure with respect to seasonal variations in temperature.

Influence of Temperature Variation on Vertical Pressures and Deformations

In this study, data collected from the pressure cells and inclinometers during the 4-year time interval (2012–2015) was used to study the influence of seasonal temperature changes on the soil–geofoam bridge approach embankment. Figure 3 presents the seasonal temperature variations from 2012 to

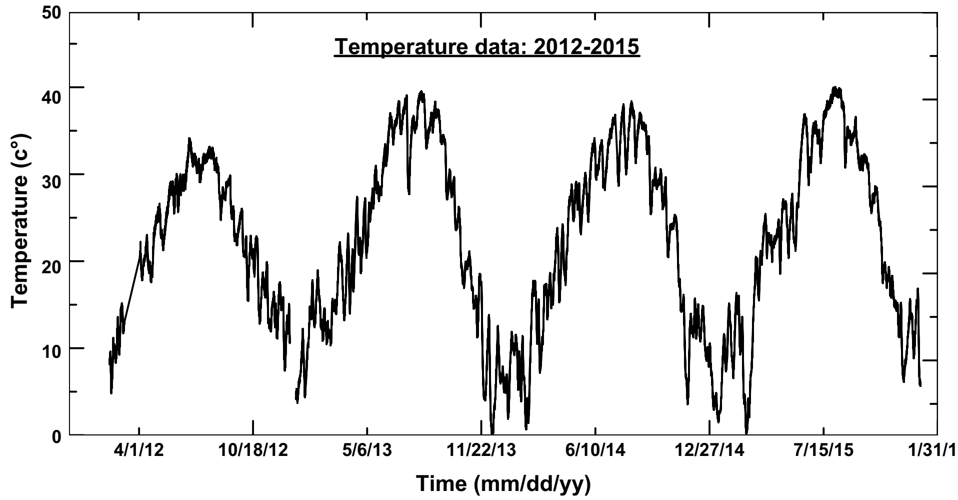

Fig. 3 Seasonal temperature variations from 2012 to 2015

2015. It can be observed that the test site under consideration has experienced temperatures ranging from 0 to 40 °C. It is evident from the figure that the rate of increase in temperature was higher for each successive year, where year 2015 has experienced several abrupt changes.

Figure 4a, b represents the typical variation of vertical pressures and temperatures during spring and summer season. It can be observed that the vertical pressures increased consistently with an increase in temperature and decreased gradually with a decrease in the temperature. Figure 5a, b present the variations in vertical pressures and deformations for each successive year. It is apparent from Fig. 5a that with an increase in temperature, vertical pressures tended to increase and decreased with the decrease in the temperature. It should be noted that the vertical pressures recorded at the bottom of the geofoam layer include pressures from the dead load (weight of the pavement structure and the geofoam) and live load (dynamic traffic load) along with temperature induced pressures. The primary reason for consistent behavior between the monitored vertical pressures and temperature variations can be related to the thermoplastic behavior of the EPS geofoam material. It should be noted that with an increase in temperature, the oxygen level will be reduced and the geofoam material tends to become viscous toward liquid phase. This

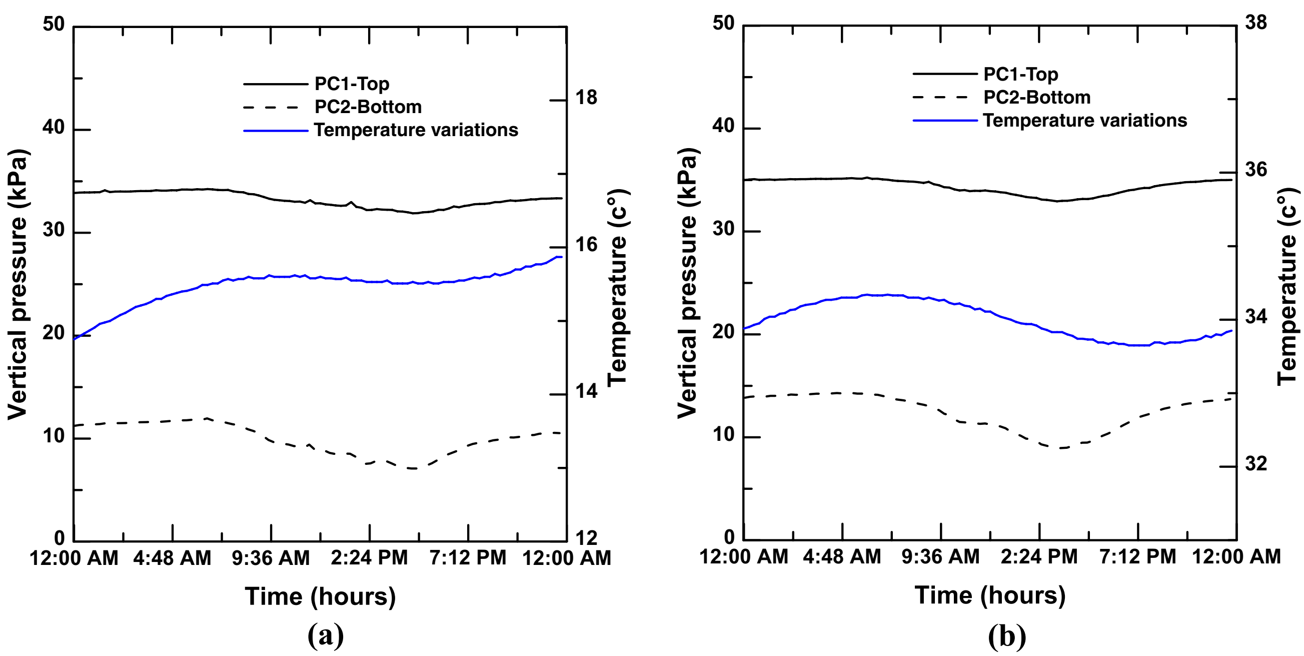

Fig. 4 Typical 1 day vertical pressures at the top and bottom of the geofoam: **a** 03/28/2013, **b** 06/05/2014

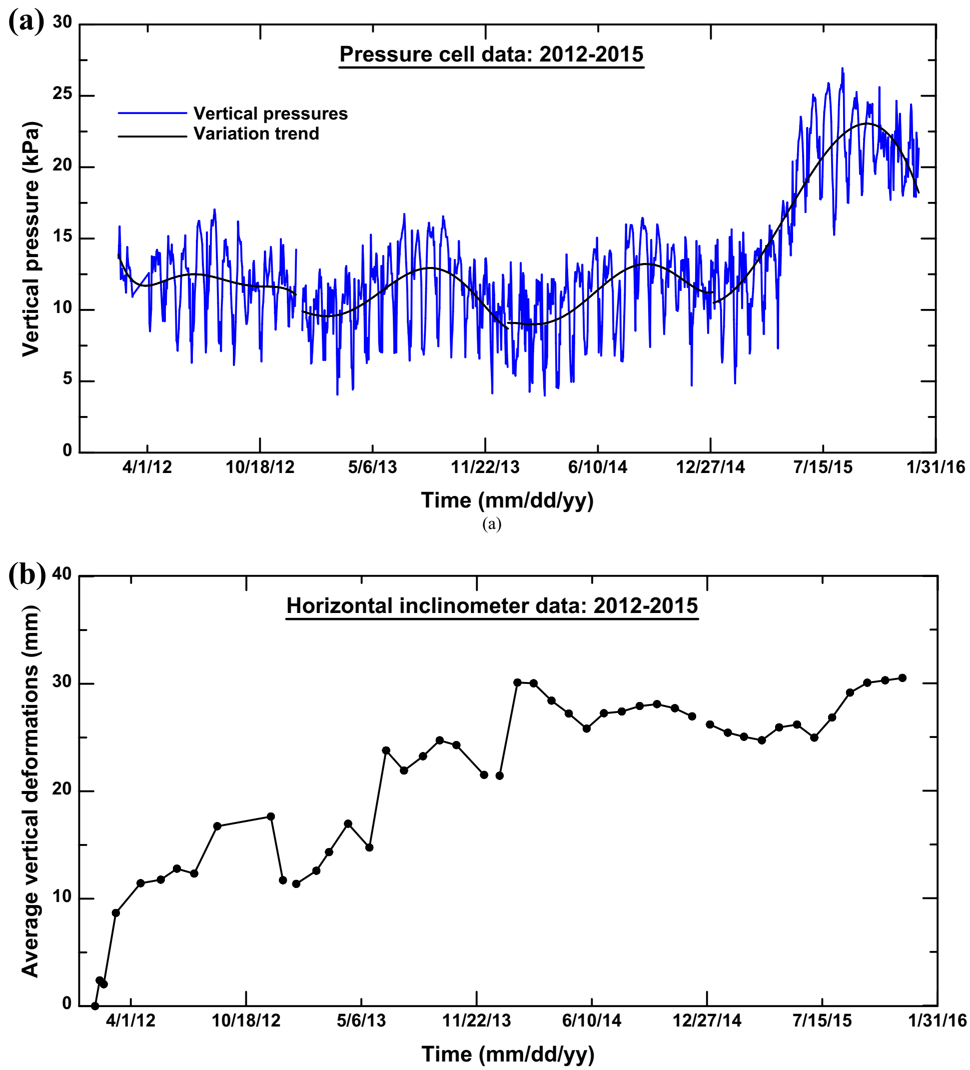

Fig. 5 **a** Average vertical pressure and **b** average vertical deformations from 2012 to 2015

thermoplastic behavior nature of EPS geofoam can lead to a decrease in the compressive strength of the material [37].

Further analysis on the effect of the temperatures on the vertical deformations (see Fig. 5b) depicted that with an increase in temperature, the deformation was increased. Conversely, a decrease in temperature during the second half of each year resulted in the decrease in deformations. This could potentially represent the swell–shrink mechanism of the expansive plastic clays at the bottom of the geofoam blocks. In order to provide further insight of this mechanism, a detailed analysis was performed for each year individually with respect to temperature changes and vertical deformations and is presented in Fig. 6a–d. It can be inferred from the plots that the seasonal temperature variations have a cyclic effect on the vertical deformations. A general trend in temperature for a complete year depicts that the temperatures increase from February till August and thereafter gradually decrease. With an increase in temperature, the settlement increased, and with a decrease in the temperature, the settlement decreased. Also, in few months, although the temperature increased, a decrease in the settlement was observed and by a decrease in the temperature, the settlement increased. A detailed analysis of other probable effective factors showed that in addition to the temperature effects, precipitation at the site also made an important contribution to the vertical deformations recorded in the field. Table 2 presents the average precipitation recorded from 2012 to 2015.

From the temperature and precipitation data, it can be inferred that the monitored vertical settlements are a result of the coupled phenomena. For instance, in the months of June and July 2012 in Fig. 6a, the settlement decreased while the temperature increased. The primary reason was due to the 162 mm (6.38 in.) of collective rainfall during the months of May and June 2012 (see Table 2). Hence, a heaving mechanism (swell) in the embankment and foundation soils due to rainfall could explain the decrease in settlement with an increase in the temperature.

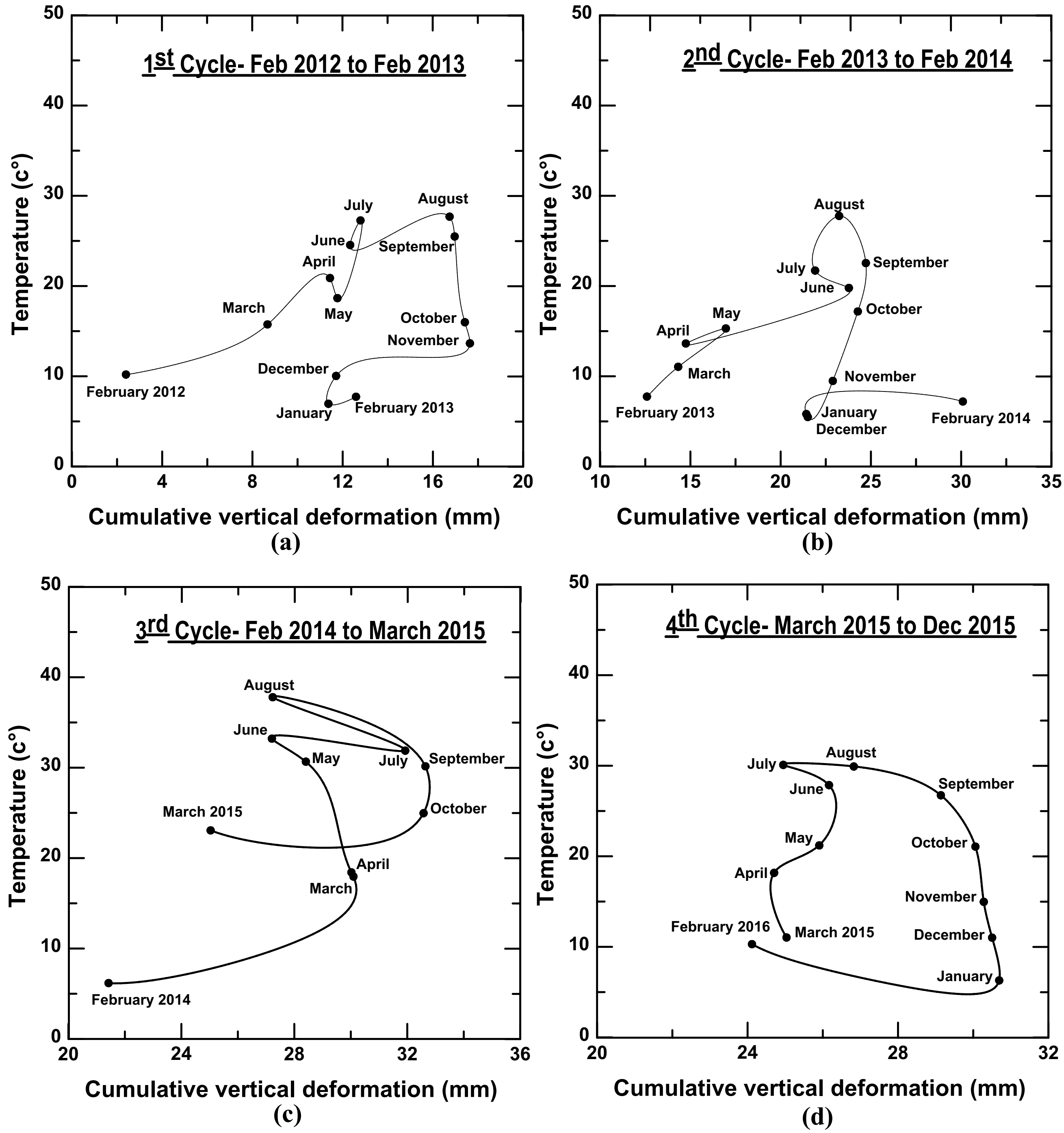

Fig. 6 Temperature variation effects on the vertical movements: **a** 1st cycle; **b** 2nd cycle; **c** 3rd cycle; **d** 4th cycle

During the months of July and August 2012, there was a decrease in the rate of the rainfall and an increase in the temperature which caused the shrinkage of the embankment and foundation soil. It was observed that the vertical pressures from the pavement structure and traffic loading remained constant from 2012 to 2015. The rapid vertical movements observed in the vertical deformation plots can be explained by the swell–shrink related volume changes of the moderately plastic clayey soils as the EPS geofoam is a homogeneous rigid material which will not have any significant swell–shrink effect [41]. At the end of each temperature-vertical deformation cycle, the residual annual settlement was observed in addition to the shrinkage settlements. Table 3 presents the annual residual settlements along

Table 2 Monthly precipitation data from 2012 to 2015

Month	Average precipitation, mm (in.)			
	2012	2013	2014	2015
January	172.2 (6.8)	95.8 (3.8)	0 (0)	95.2 (3.7)
February	65.3 (2.6)	30.7 (1.2)	9.4 (0.4)	24.6 (1)
March	112.2 (4.4)	56.1 (2.2)	15 (0.6)	72.1 (2.8)
April	14.2 (0.6)	78 (3.1)	30 (1.2)	268 (10.6)
May	82.8 (3.3)	103.4 (4.1)	184.1 (7.2)	377.2 (14.9)
June	79.2 (3.1)	19.3 (0.8)	171 (6.7)	36.8 (1.4)
July	31.7 (1.2)	79.5 (3.1)	18.3 (0.7)	0 (0)
August	28.2 (1.1)	0 (0)	69 (2.7)	36.8 (1.4)
September	106.7 (4.2)	113.5 (4.5)	4.5 (0.2)	37.3 (1.5)
October	11.9 (0.5)	101.1 (4)	62.4 (2.5)	342.9 (13.5)
November	0 (0)	51.5 (2)	59.7 (2.4)	181.8 (7.2)
December	26.9 (1.1)	0 (0)	28.4 (1.1)	52 (2)

with the precipitation records from 2012 to 2015. Annual precipitation and the average temperatures were collected from the U.S. Climate database from the weather station closest to the site.

The data from Table 3 shows a significant increase in the annual precipitation in 2015 which resulted in a considerable decrease in the settlements. Even though the average dry time periods, number of the dry cycles, and the average temperature during the dry periods are different for each year, the annual precipitation makes a dominant contribution for the residual settlements. A consistent inverse relationship is evident for the residual settlements with the annual precipitation data from 2012 to 2015.

Influence of Temperature Variation on Lateral Pressures

This section presents the analysis performed to study the effect of the seasonal temperature variations on the lateral pressures subjected on the state of the physical interaction on the inside of the bridge abutment against the geofoam. A comprehensive analysis was performed on the 4 years of data collected from 2012 to 2015. Both pressure cells were calibrated and set to zero once after they were installed laterally in the static equilibrium condition and absolute contact with both geofoam blocks and retaining walls. Thus, negative values represent a decrease in the initial lateral pressure, and positive magnitudes depict the compressive interaction between the bridge structure and the geofoam blocks. It was observed that the pressure cell installed horizontally at the top of the geofoam-retaining wall interface started to record negative values occasionally from August 2012. However, the pressure cell on the inside of the wing wall recorded only

Table 3 Annual accumulative settlements and precipitations from 2012 to 2015

Year	Annual precipitation mm (in.)	Average high temperature during dry period °C (°F)	Average dry time period (weeks)	Number of dry period cycles	Accumulative settlement mm (in.)
2012	731.5 (28.8)	21.6 (70.9)	6	1	9.3 (0.37)
2013	728.9 (28.7)	34.4 (93.9)	8	1.5	10.1 (0.4)
2014	652.0 (25.7)	13.9 (57)	7	2	11.1 (0.44)
2015	1525.0 (60)	33.1 (91.6)	6	2	5.4 (0.2)

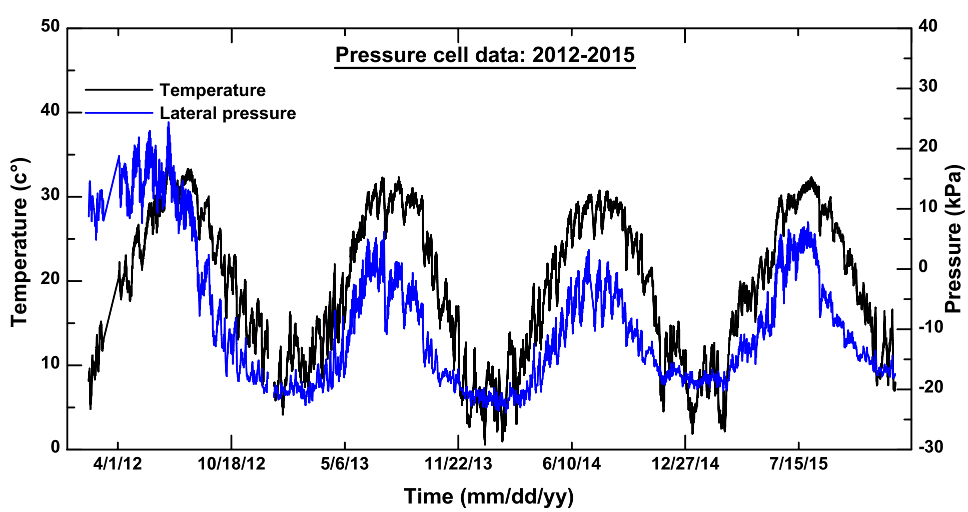

Fig. 7 Temperature and lateral pressure variations from 2012 to 2015

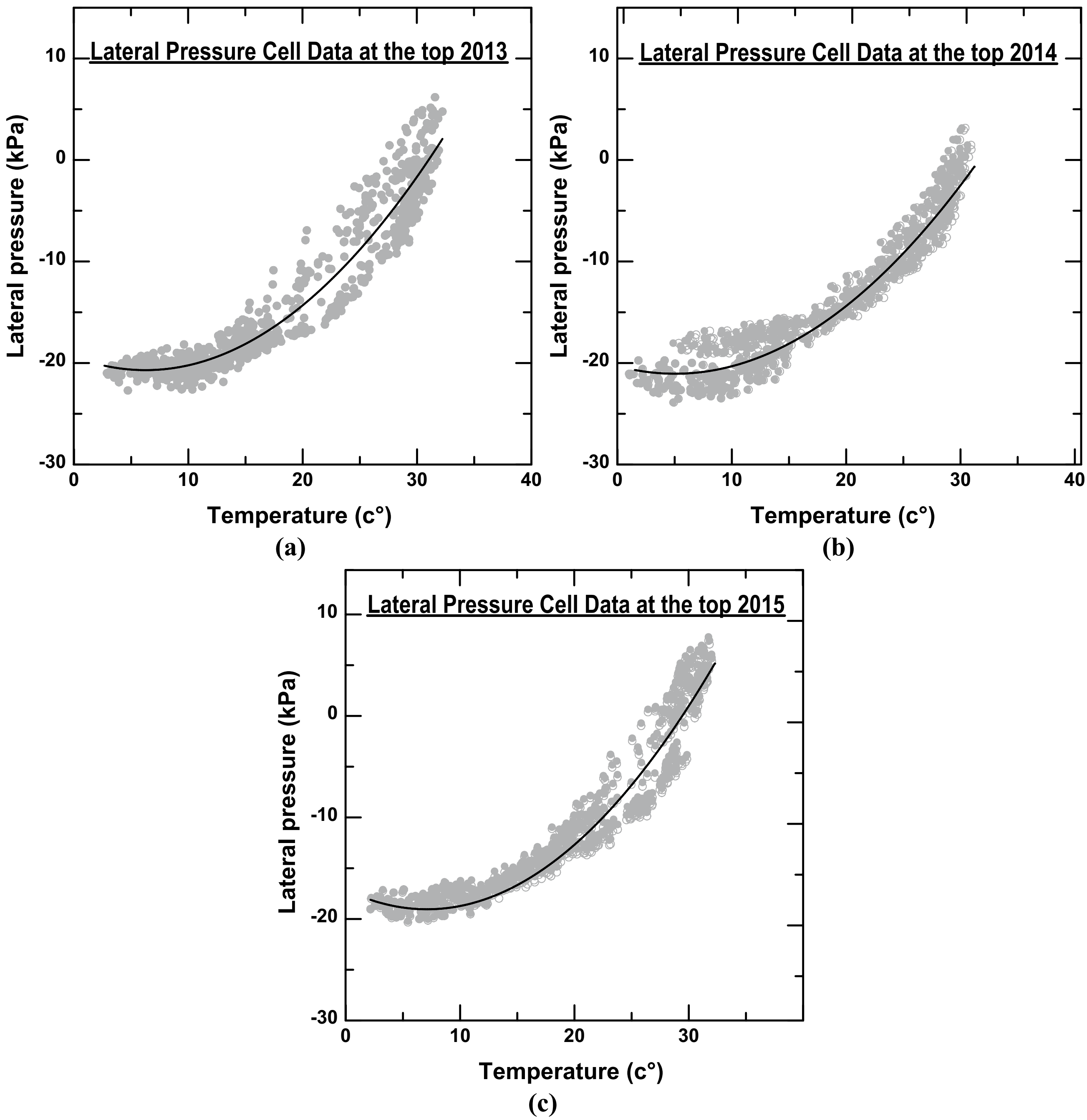

Fig. 8 Lateral pressure variation with seasonal temperature changes: **a** 2013; **b** 2014; **c** 2015

negative values which could be due to loss of contact with either the retaining wall or the geofoam blocks. Only the collected data from the pressure cell shown in Fig. 2c was used to perform the analysis. Figure 7 represents the lateral pressure and corresponding temperature variations for the data collected over the 4 years (2012–2015).

From Fig. 7, it can be inferred that in all years, the lateral pressures started to increase with an increase in temperature and decreased with a decrease in temperature. Since the lateral pressures are due to the movements in the bridge infrastructure, an attempt was made to model the variation in temperature and lateral pressure data. Figure 8 presents the pressure variation along with the temperature recorded for three consecutive years from 2013 to 2015. It was observed that the pressures were increased by increasing the temperature. The solid line depicts the best-fit line explaining the trend of the data. It can be observed that the temperature variations play a significant role in both the lateral and vertical pressures. Overall, the performance of the geofoam has resulted in a significant decrease in a vertical settlement resulting in the bump magnitudes being smaller in this embankment section.

Conclusion

A cyclic effect of seasonal temperature changes was observed on the pressures and vertical deformations measured at the bridge infrastructure. It was observed that the settlement increased with an increase in temperature, and decreased with a decrease in temperature. This trend can be related to the swell–shrink behavior of high plastic clayey soils of the embankment and foundation soils. Also, the pressure cells installed at the bottom of the geofoam layer depicted that the vertical pressures increased with an increase in temperature and decreased with a decrease in temperature. This can be attributed to the thermoplastic behavior of the EPS geofoam material. Besides reducing the overburden pressures, the geofoam can be considered as an effective technique to mitigate the bridge approach slab settlement.

Acknowledgements This study was sponsored by the Texas Department of Transportation (TxDOT) under Project No. 5-6022-03. The authors would like to acknowledge Richard Williammee, Joe Adams and other project committee members for providing their assistance with various project activities related to construction, instrumentation, and monitoring. We would also like to acknowledge the former graduate students and the colleagues for providing their assistance in the data collection.

References

1. Ruttanaporamakul P, Puppala AJ, Pedarla A, Bheemasetti TV, Williammee RS (2016) Settlement mitigation of a distressed embankment in Texas by utilization of lightweight EPS geofoam material. In Transportation Research Board 95th Annual Meeting (No. 16-4179)
2. Briaud JL, James RW, Hoffman SB (1997) NCHRP synthesis 234: settlement of bridge approaches (the bump at the end of the bridge). Transportation Research Board, National Research Council, Washington, D.C.
3. Nicks JE, Briaud JL (2007) Preliminary evaluation of the bump at the end of the railway bridge. In: Proceedings of the 2007 ASME/IEEE Joint Rail Conference and the ASME Internal Combustion Engine Division, March 13, 2007-March 16 (pp 227–240)
4. Hopkins TC (1969) Settlement of highway bridge approaches and embankment foundations. Report No. KYHPR-64-17; HPR-1(4), Kentucky Transportation Center, Lexington
5. Seo JB (2005) The bump at the end of the bridge: an investigation. Doctoral Dissertation, Texas A&M University
6. Yasrobi SY, Ng KW, Edgar TV, Menghini M (2016) Investigation of approach slab settlement for highway infrastructure. Transp Geotech 6:1–15
7. Thiagarajan G, Gopalaratnam V, Halmen C, Ajgaonkar S, Ma S, Gudimetla B, Chamarthi R (2010) Bridge approach slabs for Missouri DOT: looking at alternative and cost efficient approaches (No. OR 11.009)
8. Saride S, Puppala AJ, Archeewa E (2009) Bridge approach settlements—an issue due to design or construction practices? The University of Texas at Arlington, pp 210–214
9. White DJ, Mekkawy MM, Sritharan S, Suleiman MT (2007) “Underlying” causes for settlement of bridge approach pavement systems. J Perform Constr Facil 21(4):273–282
10. Stewart CF (1985) Highway structure approaches. FHWA/CA/SD-85-05. California Department of Transportation, Sacramento
11. Puppala AJ, Saride S, Archeewa E, Nazarian S, Williammee R Jr (2010) Bridge approach settlements: lessons learned from present case studies and ground improvement solutions. Ground Improvement and Geosynthetics (pp 228–238)
12. Tadros MK, Benak JV (1989) Bridge abutment and approach slab settlement. Phase 1. Final report (No. RES1 (0099) P433)
13. Wahls HE (1990) Design and construction of bridge approaches, vol 159. Transportation Research Board
14. Mahmood IU (1991) Evaluation of causes of bridge approach settlement and development of settlement prediction models
15. Kramer SL, Sajer P (1991) Bridge approach slab effectiveness. Final technical report (No. WA-RD 227.1)
16. Puppala AJ, Saride S, Archeewa E, Hoyos LR, Nazarian S (2009) Recommendations for design, construction, and maintenance of bridge approach slabs: synthesis report. Rep 6022–6021
17. Chen YT, Chai YH (2010) Experimental study on the performance of approach slabs under deteriorating soil washout conditions. J Bridge Eng 16(5):624–632
18. Farnsworth CB, Bartlett SF, Negussey D, Stuedlein AW (2008) Rapid construction and settlement behavior of embankment systems on soft foundation soils. J Geotech Geoenviron Eng 134(3):289–301
19. Nicks JE (2009) The bump at the end of the railway bridge. Doctoral dissertation, Texas A&M University
20. Long J, Olson S, Stark T, Samara E (1998) Differential movement at embankment-bridge structure interface in Illinois. Transp Res Rec 1633:53–60
21. Mishra D, Tutumluer E, Stark TD, Hyslip JP, Chrismer SM, Tomas M (2012) Investigation of differential movement at railroad bridge approaches through geotechnical instrumentation. J Zhejiang Univ Sci A 13(11):814–824
22. Horvath JS (2000) Integral-abutment bridges: problems and innovative solutions using EPS geofoam and other geosynthetics. Res. Rpt. No. CE/GE-00-2
23. Horvath JS (2005) Integral-abutment bridges: geotechnical problems and solutions using geosynthetics and ground improvement. West Virginia University
24. Dupont B, Allen DL (2002) Movements and settlements of highway bridge approaches, Kentucky Transportation Center. Research report, KTC-02-18/SPR-220-00-1F
25. Abu-Hejleh N, Hanneman D, White DJ, Wang T, Ksouri I (2006) Flowfill and MSE bridge approaches: performance, coast, and recommendations for improvements (No. CDOT-DTD-R-2006-2). Colorado Department of Transportation, Research Branch
26. Hsi J (2008) Bridge approach embankments supported on concrete injected columns. GeoCongress 2008: geosustainability and geohazard mitigation, pp 612–619
27. Bartlett SF, Lawton EC, Farnsworth CB, Newman MP (2012) Design and evaluation of expanded polystyrene geofoam embankments for the I-15 reconstruction project, Salt Lake City, Utah (No. UT-12.19)
28. Bartlett S, Negussey D, Kimble M, Sheeley M (2000) Use of geofoam as super-lightweight fill for I-15 reconstruction. In:

Proceedings of the Transportation Research Board 79th Annual Meeting. Transportation Research Board, Washington, DC
29. Negussey D, Stuedlein AW (2003) Geofoam fill performance monitoring. Utah Dept. of Transportation, Rep. No. UT-3
30. Newman MP, Bartlett SF, Lawton EC (2009) Numerical modeling of geofoam embankments. J Geotech Geoenviron Eng 136(2):290–298
31. Stark TD, Arellano D, Horvath JS, Leshchinsky D (2004) Geofoam applications in the design and construction of highway embankments (No. NCHRP Project 24-11)
32. Jutkofsky W, Sung J, Negussey D (2000) Stabilization of embankment slope with geofoam. Transp Res Rec 1736:94–102
33. Koerner RM (2012) Designing with geosynthetics, vol 1. Xlibris Corporation
34. Birhan A (2014) Effect of confinement and temperature on the behavior of EPS geofoam. Doctoral dissertation, Syracuse University
35. Horvath JS (1994) Expanded polystyrene (EPS) geofoam: an introduction to material behavior. Geotext Geomembr 13(4):263–280
36. Zou Y, Leo CJ, Wong H (2013) Time dependent viscoelastic behaviour of Eps geofoam. In: Applied Mechanics and Materials, vol 330. Trans Tech Publications, pp 1095–1099
37. Zou Y, Leo CJ (2001) Compressive behavior of EPS geofoam at elevated temperatures. School of Engineering and Industrial Design, University of Western Sydney
38. Acharya R, Bheemasetti TV, Ruttanaporamakul P, Chittoori B, Puppala AJ (2014) Numerical modeling of a highway embankment using geofoam material as partial fill replacement. Geo-Congress 2014: geo-characterization and modeling for sustainability, pp 2986–2995
39. ASTM D 6817-07. Standard specification for rigid cellular polystyrene geofoam. ASTM, West Conshohocken, Pennsylvania
40. Slope Indicator (2005) Digitilt inclinometer probe. Data sheet. Durham Geo Slope Indicator. http://www.slopeindicator.com/pdf/digitilt-vertical-inclinometer-probedatasheet.pdf
41. Puppala AJ, Manosuthkij T, Nazarian S, Hoyos LR, Chittoori B (2011) In situ matric suction and moisture content measurements in expansive clay during seasonal fluctuations. Geotech Test J 35:74–82